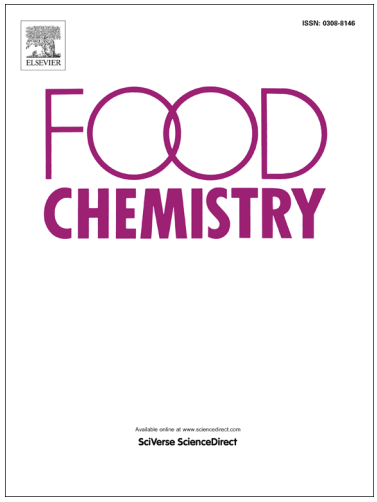

Phytosterol crystallisation within bulk and dispersed triacylglycerol matrices as influenced by oil droplet size and low molecular weight surfactant addition

Lisa M. Zychowski, Amy Logan, Mary Ann Augustin, Alan L. Kelly, James A. O'Mahony, Charlotte E. Conn, Mark A.E. Auty

PII: S0308-8146(18)30640-X
DOI: https://doi.org/10.1016/j.foodchem.2018.04.026
Reference: FOCH 22721

To appear in: *Food Chemistry*

Received Date: 5 October 2017
Revised Date: 4 April 2018
Accepted Date: 10 April 2018

Please cite this article as: Zychowski, L.M., Logan, A., Augustin, M.A., Kelly, A.L., O'Mahony, J.A., Conn, C.E., Auty, M.A.E., Phytosterol crystallisation within bulk and dispersed triacylglycerol matrices as influenced by oil droplet size and low molecular weight surfactant addition, *Food Chemistry* (2018), doi: https://doi.org/10.1016/j.foodchem.2018.04.026

Phytosterol crystallisation within bulk and dispersed triacylglycerol matrices as influenced by oil droplet size and low molecular weight surfactant addition

Lisa M. Zychowski[†§‡#], Amy Logan*[‡], Mary Ann Augustin[‡], Alan L. Kelly[§], James A. O'Mahony[§], Charlotte E. Conn[#], Mark A. E. Auty*[†]

[†] Food Chemistry and Technology Department, Teagasc Food Research Centre, Moorepark, Fermoy, Co. Cork, Ireland

[§] School of Food and Nutritional Sciences, University College Cork, Cork, Ireland

[‡] CSIROFood and Nutrition, Werribee, Victoria 3030, Australia

[#] School of Applied Science, RMIT University, Melbourne, Victoria 3000, Australia

*(A.L) Mail: CSIRO Food and Nutrition, Werribee, Victoria 3030, Australia. Phone/fax: +61 (0)3 9731 3478 Email: Amy.Logan@csiro.au.

*(M.A.E.A) Mail: Food Chemistry and Technology Department, Teagasc Food Research Centre, Moorepark, Fermoy, Co. Cork, Ireland. Phone/Fax: +353 (0)25 42442 Email: mark.auty@teagasc.ie.

Abstract

Phytosterols can lower LDL-cholesterol and are frequently used by the functional food industry. However, little is known regarding how phytosterol crystallisation can be controlled, despite solubilised phytosterols having improved bioaccessibility. This study investigates phytosterol crystallisation in bulk milk fat and in model dairy emulsion systems at two average droplet sizes, 1.0 and 0.2 μm. The effect of lecithin and monoacylglycerol addition on phytosterol crystallisation for both emulsion and bulk systems was also evaluated. Results demonstrated that lecithin and monoacylglycerols enrichment into the bulk system minimised phytosterol crystallisation. However, in emulsions, phytosterol crystallisation was mainly influenced by decreasing the droplet size. Smaller emulsion droplets containing lecithin showed the greatest potential for decreasing phytosterol crystallisation and had improved physicochemical stability. This information can be employed by the functional food industry to minimise phytosterol crystallisation and possibly improve bioaccessibility.

Introduction

Phytosterols are natural plant-derived compounds found within nuts, seeds, fruits, and vegetables. Phytosterols, which are found within plant cell membranes, are structurally similar to cholesterol (found in animal cell membranes) only differing in the presence or absence of a double bond and an R group at the twenty-fourth carbon. The structural similarities between cholesterol and phytosterols allow phytosterols to reduce absorption of cholesterol by competitive solubilisation in the low-density lipoprotein (LDL) chylomicrons, which are adsorbed by the enterocyte cells in the small intestine (Ostlund, 2002). Higher levels of LDL-cholesterol are associated with coronary heart disease, cerebrovascular accidents or strokes, and gallbladder stone disease (Moreau, Whitaker, & Hicks, 2002).

While phytosterols have been found to be effective in lowering LDL cholesterol levels, their efficacy is limited by their compositional variety, physical state and dose (Carden, Hang, Dussault, & Carr, 2015; Ostlund, Spilburg, & Stenson, 1999). To detect a significant decrease in LDL cholesterol levels ≥ 1.5 g of phytosterols needs to be consumed, which is not possible without the use of medication or functional foods. Due to the low solubility of phytosterols in oil, the hydroxyl group is normally esterified at the third carbon to improve solubility (Engel & Schubert, 2005). Although esterified phytosterols are easier to formulate into food products, they have unpredictable absorption rates, leading to variations in finding from human clinical trials (Clifton, Noakes, Ross, & Nestel, 2004). This variation in absorption levels likely reflects the requirement to hydrolyse the esterified phytosterol before absorption. Phytosterol hydrolysis during digestion is subject to inter-individual variability, causing phytosterol absorption rates to vary between 40 and 96% (Carden, Hang, Dussault, & Carr, 2015).

The efficacy of phytosterols is also limited by the physical state in which they are consumed. Solubilised phytosterols have been shown to be more effective than crystalline phytosterols at lowering LDL cholesterol (Ostlund, Spilburg, & Stenson, 1999). Decreasing the crystal size and degree of crystallinity has been proven to influence phytosterol bioavailability, yet, limited research has been conducted on how to control phytosterol crystallisation within functional food systems (Ostlund, Spilburg, & Stenson, 1999).

This study seeks to reduce phytosterol crystallisation within a mixed triacylglycerol (TAG) system, which is the typical composition of most food lipids. The model TAG system chosen for the study was milk fat, which forms β polymorphs after cooling and storage. β polymorphic structures are common in foods and occur in other lipids such as palm oil, cocoa, coconut oil, and suet (Akoh & Min, 2008). In addition, the digestion process for milk fat results in extensive changes to the structure of the lipid. During digestion the original lamellar packing of milk fat is observed to transition to more complex packings including a bicontinuous cubosome formation. The high surface area associated with these organised lipid structures may improve the bioaccessibility of bioactives dispersed within the lipid matrix (Salentinig, Phan, Khan, Hawley, & Boyd, 2013). Promising research has also shown that milk enriched with phytosterols (1.8 g/day) using a proprietary crystal-retardation method can result in a 29.1 ± 4.1% reduction in LDL-cholesterol levels (Pouteau, Monnard, Piguet-Welsch, Groux, Sagalowicz, & Berger, 2003). In a previous study by the authors, the underlying mechanism of phytosterol crystallisation within milk fat matrices was examined (Zychowski, Logan, Augustin, Kelly, Zabara, O'Mahony, et al., 2016). However, to date, no work has explored possible ways to decrease phytosterol crystallisation within a milk fat system.

Thus, this work seeks to decrease phytosterol crystallisation in both bulk and emulsified milk fat systems, with a concomitant increase in phytosterol bioaccessibility, by varying the formulation and processing parameters of the phytosterol-enriched system. Milk fat formulations were produced with or without added phytosterols and/or low molecular weight surfactants, phospholipids from lecithin or monoacylglycerol (MAG). All lipid formulations were studied in bulk milk fat, and were emulsified with whey protein isolate at two different homogenisation pressures to create droplets approximately 1.0 or 0.2 μm in diameter. Lecithin and MAG were chosen as they have been shown to impact the formation, growth, and location of crystalline compounds within oil-in-water systems (Bin Sintang, Danthine, Brown, Van de Walle, Patel, Tavernier, et al., 2017; Li, Zheng, Xiao, & McClements, 2012). Engel and Schubert (2005) demonstrated that lecithin and MAG decrease phytosterol crystallisation in both bulk and emulsion systems. However, in this study, detection of crystalline phytosterols was via polarised light microscopy, and their findings may therefore have been limited by the detection limits of the light microscope. As recent studies have demonstrated that phytosterol crystals can be as small as 36.88 Å nm in size and thus higher resolution imaging techniques and analytical tools, such as X-ray diffraction, are required to effectively quantify the level of crystallinity (Bin Sintang, et al., 2017).

Droplet size selection (~1.0 and 0.2 μm) was based on previous research demonstrating that milk fat-based, sub-micrometer-sized (<400 nm) emulsion droplets were successful in limiting the crystallisation of β-carotene (Zhang, Hayes, Chen, & Zhong, 2013); results from this study will increase our fundamental understanding of the impact of droplet size and addition of surfactants on phytosterol crystallisation within bulk and emulsion systems. This information could potentially benefit the food industry in development of functional food products with increased bioaccessibility.

2. Materials and methods

2.1 Chemicals and ingredients

Crystalline phytosterol consisting of β-sitosterol (≥70%), with residual campesterol and β-sitostanol, was purchased from Sigma Aldrich (Wicklow, Ireland). Glass capillaries with a wall thickness of 0.1 mm were purchased from Charles-Supper (Natick, Massachusetts) for synchrotron analysis. Soy lecithin (Adlec) was kindly donated by Archer Daniels Midland Co. (Chicago, Illinois) and distilled monoglycerides (Dimodan R-T PEL/B Kosher) were purchased from Danisco Australia Pty Ltd. (Banks Meadow, Australia). Whey protein isolate (WPI) (ALACEN© 895, protein content 92.0%) was obtained from Fonterra (Maungaturoto, New Zealand), sodium azide was purchased from Sigma Aldrich (Castle Hill, Australia) and commercial grade anhydrous milk fat was purchased from Marsh Dairy Product (Footscray, Australia; Table S1). For polarised images taken in Ireland at the National Imaging Centre, anhydrous milk fat was purchased from Corman Miloko (Carrick on Suir, Ireland).

2.2.1 Preparation of bulk and emulsion samples

Bulk anhydrous milk fat was combined with or without lecithin or MAG at 3% wt/wt. The bulk mixture was then heated to 110 °C while stirring on a magnetic hot plate at 300 rpm. Once a temperature of 110 °C was achieved, phytosterols were added at 3 and 6% and the mixture was stirred for 2 min. A bulk mixture of each formulation without phytosterols was also made and was subjected to the same thermal and shear treatment. After the holding period, the oil was cooled to 80 °C before loading into capillaries or glass slides for synchrotron analysis or polarised light microscopy, respectively. Samples were then allowed to cool statically to 4 °C and held at this temperature for 48 h.

Oil-in-water emulsions (10% oil: 1% protein: 89% H_20) were prepared by homogenising the described milk fat-based formulations with an aqueous protein phase. The aqueous phase was created by reconstituting whey protein isolate (WPI) at 11.11% protein with stirring at 600 rpm in an ice bath. After 2 h, the solution was then refrigerated at 4 °C overnight to allow for complete hydration. Before homogenising the two phases, aliquots of WPI solution were heated to 55 °C for 20 min. After heating, the WPI solution was mixed with Milli-Q water at 70 °C to create a 1% protein solution. This process, as employed previously, was utilised to minimise denaturation of the whey protein caused by excessive heating or high temperatures (McClements, 2004; Zychowski, et al., 2016).

The two phases were first combined into a pre-emulsion utilising a Silverson rotor-stator mixer set at 3200 rpm for 1 min. The mixture was then homogenised with an EmulsiFlex-C5 (Avestin, Mannheim, Germany) with two different processes. Larger emulsion droplets (~1.0 µm in average diameter) were generated with 1 pass at 300 bar pressure, while smaller droplets (~0.2 µm in average diameter) required 3-5 passes (depending on the formulation) at 1000 bar (Fig. S1). All emulsions were homogenised at 60 °C and then cooled and stored at 4 °C. After cooling, 0.02% of sodium azide was added to each emulsion to prevent microbial growth.

2.2.2 Synchrotron X-ray analysis.

Scattering experiments were performed on the small- and wide-angle X-ray scattering (SAXS/WAXS) beamline at the Australian Synchrotron (Clayton, Australia) with a camera length of 0.9 m and a beam of wavelength λ= 0.89 Å (14.0 keV). A Dectris Pilatus 1M captured small-angle measurements (q = 0.017-1.18 $Å^{-1}$), while a Pilatus 200K detector recorded wide-angle measurements (q = 0.95-3.19 $Å^{-1}$) (Kirby, Mudie, Hawley, Cookson, Mertens, Cowieson, et al., 2013). Samples were taken from a refrigeration unit directly into a

pre-cooled capillary holder at 4 °C. Samples equilibrated at 4 °C for 10 min before SAXS and WAXS patterns were collected. A series of three, 3 s shots were taken for each emulsion in duplicate capillaries over a 15 mm gap. Snapshots of the material references were also collected on the crystalline phytosterol (with and without MilliQ water), the aqueous phase with WPI, the lecithin and MAG after storage at 4 °C for 24 h. The beamline was calibrated using silver behenate and all diffractions patterns of averaged shots were background-subtracted using the Australian Synchrotron SAXS/WAXS software (ScatterBrain, V2.71, Australia). Bulk and emulsion diffraction peaks were analysed utilising Gaussian peak analysis (eq 1) with MatLab (Math Works Inc., Matlab R2014b, USA).

$$f(x) = a\ \mathrm{e}^{-(x-b)^2/2c^2} \quad (1)$$

In this equation, a is the maximum height of the diffracted peak, b is the peak position, and c is the full width at half-maximum (FWHM) of the peak, as used previously for SAXS/WAXS analysis (Zychowski, et al., 2016).

2.2.3 Differential scanning calorimetry

Thermal analysis of all bulk samples was conducted using a DSC 2 STARe System (Mettler Toledo, Port Melbourne, Australia). Bulk samples were prepared as described above for synchrotron analysis, with ~19-21 mg of sample weighed into a 40 µL aluminium pan (Mettler Toledo, part number ME-27331). All sample pans were hermetically sealed and stored for 48 h at 4 °C. After storage, samples were transferred immediately to a pre-cooled pan holder to maintain temperature and loaded into the DSC chamber set to 4 °C and allowed to equilibrate for 5 min before heating from to 60 °C at 2 °C min^{-1}. This method is similar to a temperature ramp used by Truong et al. (2015), except that the heating rate was slowed from 5 °C to 2 °C min^{-1} to allow for greater resolution during the milk fat melting profile.

The DSC STARe software (version 14.0) was employed to calculate the onset temperature (T_{onset}), endset (T_{endset}), along with the maximum values for each peak. The T_{onset} of the last milk fat peak was also calculated, as it shifted due to differences in formulation. All bulk formulations were prepared and analysed in triplicate.

2.2.4 Polarised light microscopy

Bulk samples were examined using polarised light microscopy on an Olympus BX51 microscope (Olympus Corporation, Tokyo, Japan) with a 20X objective lens. Digital images were captured with ProgRes CT3 camera using Prores 2.7.7 software (Jenoptik, Wiltshire, UK). After cooling to 80 °C, bulk fat formulations (50 µl) were pipetted onto a glass slide and allowed to statically cool to room temperature and later stored at 4 °C for 48 h. Glass slides were taken directly from storage onto a pre-cooled Linkam LNP heating/cooling stage at 4 °C for imaging (Linkam, Surry, UK). After imaging at 4 °C, samples were heated at 2 °C min^{-1} to observe the melting profile of the samples. Crystalline material is birefringent under polarised light and appears bright on the micrographs (Li, Zheng, Xiao, & McClements, 2012; Maher, Auty, Roos, Zychowski, & Fenelon, 2015).

2.2.5 Particle size

The particle size of the emulsion droplets was evaluated using laser light scattering on a Mastersizer 2000 instrument (Malvern Instruments Ltd., Worcestershire, UK), as described previously (Zychowski, et al., 2016). Particle size analysis was conducted in duplicate on triplicate emulsion trials for each formulation.

2.2.6 Optical characterisation of emulsion stability

Emulsion stability was analysed using a light-scattering optical analyser (Turbiscan MA2000, Formulaction, France) as a function of time. After cooling to 4 °C, 6 mL aliquots of each

emulsion were pipetted into glass holding cells and measured for backscattering at d 0. Samples were then held at 4 °C and measured after 1-week and 1-month.

Optical analysis was performed by backscattering light along the length of the glass holding cell containing the emulsion sample. This scattering data was then interpreted by a near infrared diode for the differences in optical clarity at the bottom and top of the cell, and plotted as backscattering vs. distance in the cell for each sample. Maximum backscattering values for each treatment were compared against those of day 0 to evaluate the change in emulsion stability during storage, as described previously (Zychowski, et al., 2016).

2.2.6 Statistical Analysis.

For analysis of emulsion and bulk formulations, mean values ± standard deviations were presented. All results were analysed utilizing SAS® 9.3 software for Windows (Cary, North Carolina). A Tukey's Post Hoc Difference Test with a level of probability at $p<0.05$ was employed to analyse significant differences between treatments.

3.0 Results and Discussion

3.1 The effect of lecithin or MAG on phytosterol and milk fat crystallisation within bulk systems

The structural behaviour of different bulk milk fat formulations, with and without phytosterols, was determined using Synchrotron SAXS/WAXS, DSC measurements, and polarised light microscopy. Synchrotron SAXS/WAXS data was utilised to assess the presence of phytosterol crystals by comparing diffraction patterns of the bulk milk fat formulations to the crystalline phytosterol and material diffraction patterns (Fig. 1). Figure 1.1a shows the SAXS diffraction pattern from the bulk and emulsified milk fat. The spectrum is characteristic of a double lamellar (2L) structure, regardless of whether the milk fat is in a

bulk or emulsified form, consistent with previous (Akoh & Min, 2008). The corresponding WAXS (Fig. 1.1b) patterns demonstrate the polymorphic structures formed by the milk fat and will be discussed in more detail below.

Spectra were also collected for phytosterol both as a dry powder and 5% wt/wt aqueous dispersion (Fig. 1.2a-b). The crystalline phytosterol powder is most likely composed of one or more β-sitosterol polymorphs including hemihydrated, anhydrous, and/or monohydrated crystals, as observed by Moreno-Calvo et al. (2014) for a similar phytosterol mixture. When dispersed in water, fewer diffraction peaks were observed compared to the dry powder (peaks 1, 2, 6 and 7 only). The difference in phytosterol diffraction observed between the dry and aqueous dispersed powder is most likely due to the main phytosterol, β-sitosterol, maintaining only the monohydrated and/or hemihydrated crystal polymorphs (Bin Sintang, et al., 2017). Similar results were also observed by Christiansen et al. (2002), where X-ray diffraction patterns of β-sitosterol dispersed within oil were altered by the addition of water to the systems. As the phytosterol powder is a mixture of phytosterols, it is difficult to determine the exact phytosterol crystal varieties present within the system. However, a higher number of phytosterol peaks has previously been found to be related to a higher amount of crystalline phytosterols (von Bonsdorff-Nikander, Karjalainen, Rantanen, Christiansen, & Yliruusi, 2003).

The pure MAG powder was also evaluated to assess the presence of crystalline material within the sample under dry and aqueous dispersed conditions (Fig. 1.3a-b). Unlike the powdered phytosterol, the MAG powder was found to produce similar SAXS and WAXS spectra, characteristic of a lamellar phase, with and without water, consistent with previous research (Qiu & Caffrey, 2000). Lecithin was similarly evaluated (data not shown), but

produced no Bragg peaks indicating a lack of long range structural order (Akoh & Min, 2008).

For mixtures consisting of milk fat and phytosterol, milk fat peaks dominated the sample spectra. At 6% phytosterol enrichment, 10 separate lattice distances could be detected from phytosterol crystals; 35.6, 17.7, 11.7, 9.7, 8.8, 7.4, 5.9, 5.2, 4.8, and 4.7 Å (Fig. 2c-d & Table 1). At 3% phytosterol enrichment in bulk milk fat, only 4 of the 10 phytosterol crystalline peaks observed at 6% enrichment were present, indicating that lower phytosterol concentrations can influence the number and intensity of the phytosterol crystal peaks, as observed previously (von Bonsdorff-Nikander, Karjalainen, Rantanen, Christiansen, & Yliruusi, 2003). Upon addition of both lecithin and MAG, phytosterol crystallisation was suppressed in the 3% enriched formulation, as determined by a reduction in the number and intensity of phytosterol peaks observed (Fig. 2a-b). While crystal formation persisted in the 6% sample, only 8 out of the 10 phytosterol diffraction peaks were observed, potentially indicative of a reduction in the amount of crystalline phytosterols (Fig. 2c-d).

This high-resolution Synchrotron SAXS data confirms the microscopy observations performed by Engel et al. (2005), which indicated that lecithin (a phospholipid) and MAG could reduce the crystallisation of phytosterols when added to a bulk TAG system by acting as a solubility aid. In nature, phospholipids associate with and help solubilise phytosterols within plant cell membranes, contributing to the fluidity of the membrane (Dufourc, 2008). The affinity of sterols with phospholipids is also applicable to mammalian cells; interactions between cholesterol and phospholipids are necessary for cholesterol solubilisation (Ohvo-Rekilä, Ramstedt, Leppimäki, & Peter Slotte, 2002). Previous work has also shown that sitostanol, the saturated form of sitosterol, can be solubilised within ultrasonicated lecithin micelles. Interestingly, these lecithin-containing sitostanol-micelles were able to reduce

cholesterol ~25% more effectively in humans than the powdered crystalline sitostanol, again emphasising the importance of solubilising plant sterols before ingestion (Ostlund, Spilburg, & Stenson, 1999).

We suggest that, in addition to phytosterol solubilisation effects, the polar head groups of the phospholipid molecules could have influenced the development of the milk fat TAG network by means of steric hindrance. Previous work on mixtures of milk fat and lecithin demonstrated that lecithin is able to delay the induction of milk fat crystallisation (Vanhoutte, Foubert, Duplacie, Huyghebaert, & Dewettinck, 2002). Vanhoutte et al. (2002) hypothesised that phospholipids incorporate themselves within the crystallisation nuclei during the initial phase of crystallisation, blocking crystal growth, as subsequent TAG attachment is slowed by the physical presence of the bulky phospholipid molecule.

Thermal outputs captured from DSC measurements during heating showed a significant ($p < 0.05$) decrease in the melting enthalpy of all samples containing lecithin, with or without added phytosterols (Table 1). The energy released during melting demonstrates that some milk fat tended to crystallise upon storage. The decrease in melting enthalpy, however, suggests that the milk fat crystalline network was indeed less developed in samples containing lecithin. In addition, polarised optical microscopy images of bulk milk fat samples enriched with lecithin possessed a less developed and non-homogenous milk fat crystal network compared to the bulk milk fat samples, with larger spherulites present throughout (Fig. 3, white arrows). The difference between the samples with and without lecithin is similar to the difference seen within milk fat samples crystallised at 25 and 4 ºC (Wright, Hartel, Narine, & Marangoni, 2000). At lower temperatures, the critical radius of crystalline milk fat nuclei are smaller than at higher crystallisation temperatures, because of the decreasing solubility of the TAG molecules and the increasing free energy of the system

(Wright & Marangoni, 2006). In our study, distinct large spherulites are clearly apparent throughout the samples containing lecithin, suggesting that lecithin influenced the milk fat TAG network growth (Fig. 3). Similar results for bulk palm oil were found where the addition of lecithin-derived phospholipids increased the size of the spherulites, while reducing the total amount of palm oil TAG crystals and leading to a loss of interlocking crystals between the palm oil spherulites (Smith, 2000).

Conversely, MAG is known for initiating TAG nucleation. Here, TAG molecules adsorb onto the MAG surface and act as catalytic seed crystal impurities (Basso, Ribeiro, Masuchi, Gioielli, Gonçalves, Santos, et al., 2010). A larger number of seed crystals leads to the formation of smaller TAG crystals throughout, creating a dense crystalline network. In our work, images taken of samples enriched with MAG after storage show smaller milk fat crystals compared to the control (Fig. 3). This is consistent with previous results for other MAG-enriched TAG systems (Basso, et al., 2010; Verstringe, Danthine, Blecker, & Dewettinck, 2014). Dense crystalline networks are often used in solid-lipid nanoparticle (SLN) technology, where a solid-lipid carrier matrix entraps the bioactive. The entrapment of the bioactive in a crystalline matrix can limit the mobility of the bioactive, preventing its crystallisation and degradation (Bunjes, Drechsler, Koch, & Westesen, 2001; Helgason, Awad, Kristbergsson, Decker, McClements, & Weiss, 2009). In addition, recent research has suggested that phytosterols and MAG can form bilayer-type complexes through hydrogen bonding. Although no crystalline phytosterol and MAG complexes were observed in SAXS data, MAG and phytosterol interactions could possibly alter the phytosterol crystallisation behaviour, as observed previously (Bin Sintang, et al., 2017).

Both lecithin and MAG addition prevented phytosterol crystallisation at 3% and reduced the number of crystalline phytosterol peaks in the 6% formulation, as evident in SAXS/WAXS

diffraction patterns. Their impact on phytosterol crystallisation was also evident visually. In polarised images, phytosterols appeared as plate-like crystals, as outlined in Figure 3. No distinguishable plate-like phytosterol crystals were observed in samples enriched with either lecithin or MAG. Upon heating to 40 ºC, the crystalline networks formed within the lecithin and MAG network melted. During this heating process, the 6% phytosterol without lecithin or MAG was the only sample to have noticeable crystals present at temperatures ≥ 40 ºC (Fig. S3. The milk fat networks containing lecithin or MAG were also observed to melt differently compared to the control; at 30 ºC, a much finer crystalline network is observed which displays almost no birefringence, as opposed to the lecithin containing system where large spherulites were still visible (Fig. S3).

Regardless of lecithin or MAG addition, bulk milk fat was found to be of a double chain length (2L) configuration with a d-spacing between 39.4 and 40.1 Å after storage at 4 °C for 48 h. Both β and β' polymorphs (Table 1 & Fig. 1.1a-b) were observed to be similar to other MF systems (Bugeat, Briard-Bion et al. 2011, Truong, Morgan et al. 2015). Earlier results demonstrated that milk fat with added phytosterols forms a more disordered 3L matrix with a loose α-packing during the initial phases of the crystallisation (Zychowski, et al., 2016). Over time, the TAG network shifts from the unstable 3L α-packing to a more stable 2L form with β and β' polymorphs.

This is also the case for milk fat with MAG or lecithin, as upon 3% addition of either of these compounds no change in milk fat lamellar spacing was seen within the TAG structure after storage (Table 1). Similar results have been seen in a palm oil enriched with the MAG monopalmitin (Verstringe, Dewettinck, Ueno, & Sato, 2014). In their work, palm oil crystallisation was induced by monopalmitin molecules during crystallisation, and monopalmitin crystals were detected at palm oil nucleation sites. However, after 1-week of

storage, monopalmitin crystals migrated and crystallised separately in the interstitial spaces between palm oil crystals.

Differential scanning colorimetry was also used to examine the thermal transitions of each bulk sample, with two main differences being observed (Fig. S2 & Table 1). Firstly, phytosterol enrichment significantly ($p < 0.05$) increased the onset temperature (T_{onset}) of the high-melting point milk fat fraction in both the control and in the sample containing MAG. Earlier results demonstrated the ability of phytosterol molecules to slow the lamellar devolution of the milk fat network through steric hindrance during melting (Zychowski, et al., 2016). No effect on the T_{onset} of the high-melting point fraction was observed for samples containing lecithin. Within the lecithin enriched samples, it is also possible that the lack of milk fat TAG crystal growth minimised the effect of phytosterols on the high-melting point fraction, as an increase in the onset temperature is not distinguishable (Fig. S2 & Table 1).

3.2 The effect of emulsion droplet size on phytosterol crystallisation

Phytosterol crystallisation within the phytosterol-enriched (PE) emulsion systems was assessed as a function of phytosterol concentration (0.3 and 0.6%) and droplet size ($D_{(4,3)}$ = 0.2 and 1.0 µm average diameter, respectively) using Synchrotron SAXS/WAXS (Fig. 4 & Table 2). Results were compared to the bulk milk fat SAXS/WAXS patterns described earlier (Fig. 2 & Table 1); the number of phytosterol peaks was shown to decrease when moving from a bulk to an emulsified state with an average droplet size of 1.0 µm (Tables 1 & 2). A decrease in the number and intensity of phytosterol crystalline peaks was also observed with decreasing droplet size. For example, for the 0.3% enrichment formulation, no phytosterol peaks were detected in the 0.2 µm emulsions compared to the 4 peaks observed in the 1.0 µm emulsions. To a lesser degree, emulsion size also influenced the 0.6% enriched emulsion,

with the crystalline peak present at 35.6 Å in the 1.0 µm emulsion absent within the smaller sized emulsion.

Dispersing a lipid matrix into an oil-in-water emulsion system results in droplets with a small lipid volume, which limits the number of possible nucleation sites (McClements, 2012). During cooling, the phytosterols would be supersaturated within the bulk milk fat but, without sufficient nuclei in each droplet, the large activation energy required for nucleation can result in a metastable state (Li, Zheng, Xiao, & McClements, 2012; McClements, 2012). This metastable, supersaturated state can persist for some time, as a larger activation energy must be overcome before the crystal nuclei can form and grow into crystals. Dispersing the lipid matrix within droplets limits these nucleation sites and is even more pronounced in droplets with a smaller volume (Karadag, Yang, Ozcelik, & Huang, 2013).

Decreased crystallisation of bioactive components when comparing a bulk to an emulsion system has also been observed in other studies, due to this change in activation energy (Bunjes, Drechsler, Koch, & Westesen, 2001; Oehlke, Adamiuk, Behsnilian, Gräf, Mayer-Miebach, Walz, et al., 2014). In addition, as seen within the crystalline phytosterol powder, and its aqueous dispersed form (Fig. 1.2a-b), phytosterols form different crystalline structures in the presence of water (Christiansen et al., 2002). Phytosterols can participate in surface heterogeneous nucleation, and tend to crystallise at the surface of the emulsion droplets (Chen, Guo, Wang, Yin, & Yang, 2016; McClements, 2012; Zychowski, et al., 2016).

Crystallisation in emulsion systems may influence the physical stability of the emulsion over time (McClements, 2012). To evaluate stability, emulsions were tested for creaming (Δ backscattering) after 1-week and 1-month storage at 4 ºC, utilising a turbiscan optical analyser (Fig. S4 & Table 1). No significant change ($p<0.05$) in backscattering was observed after 1-week or 1-month of production between WPI stabilised emulsions with or without

phytosterol addition. This is despite the fact that phytosterols were found to be crystalline within these samples (Fig. 4 & Table 2). This indicates that, within this system, phytosterol crystallisation does not result in emulsion destabilisation through partial coalescence of the lipid droplets, as observed within other emulsion systems (McClements, 2012). Although uncharacteristic of emulsified crystalline material, crystalline phytosterols have previously been found to improve emulsion stability. In one such study, performed by Chen et al. (2016), phytosterols were co-crystallised with octenyl succinic anhydride starch at an emulsion interface. The resulting rigid phytosterol complex decreased droplet coalescence and improved the overall stability of the emulsion over time.

Decreasing the droplet size of an emulsion can also greatly improve the thermodynamic stability of the emulsion, and decrease the tendency for an emulsion to phase separate into lipid and aqueous phases (McClements, 2012). As expected, the 0.2 um emulsion showed a dramatic increase in emulsion stability over time at both the 1-week and 1-month mark compared to the 1 µm sample (Fig S4. & Table 2). As creaming occurred, emulsion droplets gathered at the top of the tube resulting in a clearing at the bottom. Droplet movement from the bottom of the tube is apparent by increasing line curvature from ~ 7 to 25 mm, while creaming is reflected in the increasing backscattering values at ~ 70 mm (Fig. S4). The 1.0 µm control emulsion was found to be less stable than the control formulation prepared with an average droplet size of 0.2 um. This was evident from larger backscattering values and a higher line curvature at the bottom of the tube (Fig. S4 & Table 2). Similar results regarding increases in emulsion destabilisation within larger droplet emulsion systems have been observed in other oil-in-water dispersed systems (Chanamai & McClements, 2000). Extreme changes in backscattering between the 1.0 and 0.2 µm PE emulsions demonstrate how

emulsion stability is largely affected by droplet size, and independent of phytosterol crystallisation in the emulsion droplets.

3.3 The effect of lecithin and MAG on phytosterol crystallisation and emulsion formation and stability

Phytosterol emulsions of 0.2 and 1.0 µm average droplet size were also evaluated for phytosterol crystallisation upon the addition of lecithin and MAG to the dispersed milk fat. Synchrotron SAXS/WAXS patterns demonstrated that there was no difference in the number of crystalline phytosterol peaks in the samples at 1.0 µm, even after the addition of lecithin and MAG (Table 2). However, the addition of lecithin and MAG did prevent the phytosterol peak observed at 17.7 Å in the 1.0 µm emulsion from occurring in the 0.2 µm sample at 0.6% enrichment. This minor change indicates that the most significant reductions in phytosterol crystallisation were due to a decrease in droplet size, as previously discussed (Fig. 4 & Table 2).

The 1.0 µm emulsions prepared with either lecithin or MAG had statistically similar ($p > 0.05$) $D_{(4,3)}$ values between formulations independent of phytosterol concentration, except for the emulsion stabilised by WPI alone, which showed a significant decrease in average droplet size with the addition of 0.6% phytosterol, from 0.93 ± 0.06 to 0.73 ± 0.07 µm. A similar decrease in the droplet size of WPI stabilised emulsions with phytosterol addition has been documented in previous work and is believed to be due to a synergistic interaction between phytosterols and whey protein at the oil-in-water interface. Phytosterol and whey protein can decrease interfacial tension at the oil/water interface of the system to a greater extent together, than each compound can achieve separately (Zychowski, Mettu, Dagastine, O'Mahony, & Auty, 2017). While all 1.0 µm emulsion droplets required 1 pass at 300 bar to form a stable, monomodal emulsion distribution, the phytosterol emulsion formulations with

an average of 0.2 µm sized droplets required homogenisation at 1000 bar and either 4, 3, or 5 passes for the WPI, WPI + lecithin, and WPI + MAG samples, respectively. It is interesting to note that, to create the same sized droplets, lecithin-enriched emulsions required fewer homogenisation passes, while emulsions containing MAG required more than the control stabilized with WPI alone.

During storage, the 1.0 µm WPI stabilized phytosterol emulsions showed a significant increase ($p < 0.05$) in backscattering after 1-week, compared to those stabilized with additional lecithin and MAG (Table 2). However, after 1-month, all 1.0 µm emulsions showed relatively similar changes in backscattering. This indicates that in 1.0 µm sized emulsion droplets, lecithin and MAG provided some initial enhanced stability to the system, but over time this advantage was lost. After 1-week of storage at 4 ºC, all of the 0.2 µm emulsions were statistically similar in average droplet size ($p > 0.05$) and stability (Fig S4 & Table 2). However, after 1-month, the 0.2 µm emulsions with MAG showed a significant increase ($p < 0.05$) in backscattering compared to all other formulations, and was the least stable.

This trend was not observed within the 1.0 µm PE emulsions, which could be due to the greater levels of surfactant required to stabilize the larger droplet interface in the 0.2 µm, systems, where surface area is inversely related to droplet size (Li, Zheng, Xiao, & McClements, 2012). The larger surface area could have encouraged MAG to migrate from the lipid phase to the surface in order to stabilise the emulsion. While MAG can provide stability in some emulsion systems, it is prone to crystallisation at the interface, which in turn can lead to emulsion instability (Mao, Calligaris, Barba, & Miao, 2014). In addition, previous research has demonstrated that MAG can replace WPI at an emulsion interface, even though this replacement results in a more unstable system (Mao, Calligaris, Barba, & Miao, 2014).

Finally, it is interesting to note that the 0.6% PE emulsion with 0.2 µm sized droplets and lecithin was still physically stable after 1-month (Table 2). Lecithin can aid solubility of the phytosterol in phospholipid-based membranes, and thus, it is possible that the two amphiphilic compounds could also be interacting at the emulsion interface to provide greater emulsion stability (Hąc-Wydro, Wydro, Jagoda, & Kapusta, 2007; Ostlund, Spilburg, & Stenson, 1999). Future research could investigate the relationship between the two compounds at the interface, and if higher levels of added lecithin could improve PE emulsion stability.

Summary and Conclusion

This research study sought to understand how crystallisation of phytosterols was impacted by changes within formulation and droplet size. In addition, the systems were analysed for physicochemical changes using DSC, stability testing and polarised light microscopy. In bulk fat systems, the addition of the two surfactants, lecithin and MAG, reduced phytosterol crystallisation through increasing the solubility of the phytosterols and by creating a dense crystalline network entrapping the phytosterol, respectively. Once these formulations were dispersed in emulsion systems, diffraction patterns demonstrated that reductions in phytosterol crystallisation were mostly driven by decreasing the size of the emulsion droplets, not the addition of lecithin or MAG. However, within the smaller PE emulsions with a $D_{(4,3)}$ of 0.2 µm, samples with added MAG were found to be the most unstable, while the 0.6% PE emulsion with lecithin was found to be the most stable over time. This fundamental study is important in understanding how bioactive crystallisation is driven by processing and formulation factors. This information is valuable for the functional food industry to help reduce crystallisation of phytosterols, leading to improved bioaccessibility of the bioactive within the final food product.

Author information

*(M.A.E.A.) Phone/fax: +353 (0)25 42442. E-mail: mark.auty@teagasc.ie.

*(A.L.) Phone/fax: +61 (0)3 9731 3478. E-mail: Amy.Logan@csiro.au.

Acknowledgements

The authors would like to thank the Teagasc Food Research Centre for assistance in funding this collaborative project (Teagasc Project 6412: "Structured Dairy Emulsions"), and the Australian Synchrotron for beamline access (proposal M10097). The authors would also like to acknowledge the Australian Research Council, as Dr. Charlotte Conn is the recipient of a DECRA Fellowship DE160101281. The authors are also grateful to Nigel Kirby (Australian Synchrotron, Melbourne, Australia) for his invaluable guidance in setting up the Synchrotron experiment. In addition, we thank Tamar Greaves (RMIT, Australia), Stephan Homer (CSIRO, Australia), and Lisa Blazo (University of Sheffield) for their assistance with this project.

Conflict of interest

The authors declare that there are no conflicts of interests.

References

Akoh, C. C., & Min, D. B. (2008). *Food Lipids: Chemistry, Nutrition, and Biotechnology*: CRC press.

Basso, R. C., Ribeiro, A. P. B., Masuchi, M. H., Gioielli, L. A., Gonçalves, L. A. G., Santos, A. O. d., Cardoso, L. P., & Grimaldi, R. (2010). Tripalmitin and monoacylglycerols as modifiers in the crystallisation of palm oil. *Food Chemistry, 122*(4), 1185-1192.

Bin Sintang, M. D., Danthine, S., Brown, A., Van de Walle, D., Patel, A. R., Tavernier, I., Rimaux, T., & Dewettinck, K. (2017). Phytosterols-induced viscoelasticity of oleogels prepared by using monoglycerides. *Food Research International, 100*(Part 1), 832-840.

Bunjes, H., Drechsler, M., Koch, M. J., & Westesen, K. (2001). Incorporation of the Model Drug Ubidecarenone into Solid Lipid Nanoparticles. *Pharmaceutical Research, 18*(3), 287-293.

Carden, T. J., Hang, J., Dussault, P. H., & Carr, T. P. (2015). Dietary plant sterol esters must be hydrolyzed to reduce intestinal cholesterol absorption in hamsters. *The Journal of Nutrition*.

Chanamai, R., & McClements, D. J. (2000). Dependence of creaming and rheology of monodisperse oil-in-water emulsions on droplet size and concentration. *Colloids and Surfaces A: Physicochemical and Engineering Aspects, 172*(1–3), 79-86.

Chen, X.-W., Guo, J., Wang, J.-M., Yin, S.-W., & Yang, X.-Q. (2016). Controlled volatile release of structured emulsions based on phytosterols crystallization. *Food Hydrocolloids, 56*, 170-179.

Christiansen, L. I., Rantanen, J. T., von Bonsdorff, A. K., Karjalainen, M. A., & Yliruusi, J. K. (2002). A novel method of producing a microcrystalline β-sitosterol suspension in oil. *European Journal of Pharmaceutical Sciences, 15*(3), 261-269.

Clifton, P., Noakes, M., Ross, D., & Nestel, P. (2004). High dietary intake of phytosterol esters decreases carotenoids and increases plasma plant sterol levels with no additional cholesterol lowering. *Journal of Lipid Research, 45*(8), 1493-1499.

Dufourc, E. J. (2008). Sterols and membrane dynamics. *Journal of Chemical Biology, 1*(1-4), 63-77.

Engel, R., & Schubert, H. (2005). Formulation of phytosterols in emulsions for increased dose response in functional foods. *Innovative Food Science & Emerging Technologies, 6*(2), 233-237.

Hąc-Wydro, K., Wydro, P., Jagoda, A., & Kapusta, J. (2007). The study on the interaction between phytosterols and phospholipids in model membranes. *Chemistry and Physics of Lipids, 150*(1), 22-34.

Helgason, T., Awad, T. S., Kristbergsson, K., Decker, E. A., McClements, D. J., & Weiss, J. (2009). Impact of Surfactant Properties on Oxidative Stability of β-Carotene Encapsulated within Solid Lipid Nanoparticles. *Journal of Agricultural and Food Chemistry, 57*(17), 8033-8040.

Karadag, A., Yang, X., Ozcelik, B., & Huang, Q. (2013). Optimization of preparation conditions for quercetin nanoemulsions using response surface methodology. *Journal of Agricultural and Food Chemistry, 61*(9), 2130-2139.

Kirby, N. M., Mudie, S. T., Hawley, A. M., Cookson, D. J., Mertens, H. D., Cowieson, N., & Samardzic-Boban, V. (2013). A low-background-intensity focusing small-angle X-ray scattering undulator beamline. *Journal of Applied Crystallography, 46*(6), 1670-1680.

Li, Y., Zheng, J., Xiao, H., & McClements, D. J. (2012). Nanoemulsion-based delivery systems for poorly water-soluble bioactive compounds: Influence of formulation parameters on polymethoxyflavone crystallization. *Food hydrocolloids, 27*(2), 517-528.

Maher, P. G., Auty, M. A. E., Roos, Y. H., Zychowski, L. M., & Fenelon, M. A. (2015). Microstructure and lactose crystallization properties in spray dried nanoemulsions. *Food Structure, 3*(0), 11.

Mao, L., Calligaris, S., Barba, L., & Miao, S. (2014). Monoglyceride self-assembled structure in O/W emulsion: formation, characterization and its effect on emulsion properties. *Food Research International, 58*, 81-88.

McClements, D. J. (2004). Protein-stabilized emulsions. *Current Opinion in Colloid & Interface Science, 9*(5), 305-313.

McClements, D. J. (2012). Crystals and crystallization in oil-in-water emulsions: Implications for emulsion-based delivery systems. *Advances in Colloid and Interface Science, 174*, 1-30.

Moreau, R. A., Whitaker, B. D., & Hicks, K. B. (2002). Phytosterols, phytostanols, and their conjugates in foods: structural diversity, quantitative analysis, and health-promoting uses. *Progress in Lipid Research, 41*(6), 457-500.

Moreno-Calvo, E., Temelli, F., Cordoba, A., Masciocchi, N., Veciana, J., & Ventosa, N. (2014). A New Microcrystalline Phytosterol Polymorph Generated Using CO2-Expanded Solvents. *Crystal Growth & Design, 14*(1), 58-68.

Oehlke, K., Adamiuk, M., Behsnilian, D., Gräf, V., Mayer-Miebach, E., Walz, E., & Greiner, R. (2014). Potential bioavailability enhancement of bioactive compounds using food-grade engineered nanomaterials: a review of the existing evidence. *Food & Function, 5*(7), 1341-1359.

Ohvo-Rekilä, H., Ramstedt, B., Leppimäki, P., & Peter Slotte, J. (2002). Cholesterol interactions with phospholipids in membranes. *Progress in Lipid Research, 41*(1), 66-97.

Ostlund, R. E. (2002). Phytosterols in human nutrition. *Annual Review of Nutrition, 22*(1), 533-549.

Ostlund, R. E., Spilburg, C. A., & Stenson, W. F. (1999). Sitostanol administered in lecithin micelles potently reduces cholesterol absorption in humans. *The American Journal of Clinical Nutrition, 70*(5), 826-831.

Pouteau, E. B., Monnard, I. E., Piguet-Welsch, C., Groux, M. J. A., Sagalowicz, L., & Berger, A. (2003). Non-esterified plant sterols solubilized in low fat milks inhibit cholesterol absorption. *European Journal of Nutrition, 42*(3), 154-164.

Qiu, H., & Caffrey, M. (2000). The phase diagram of the monoolein/water system: metastability and equilibrium aspects. *Biomaterials, 21*(3), 223-234.

Salentinig, S., Phan, S., Khan, J., Hawley, A., & Boyd, B. J. (2013). Formation of highly organized nanostructures during the digestion of milk. *American Chemical Society Nano, 7*(12), 10904-10911.

Truong, T., Morgan, G. P., Bansal, N., Palmer, M., & Bhandari, B. (2015). Crystal structures and morphologies of fractionated milk fat in nanoemulsions. *Food Chemistry, 171*, 157-167.

Vanhoutte, B., Foubert, I., Duplacie, F., Huyghebaert, A., & Dewettinck, K. (2002). Effect of phospholipids on isothermal crystallisation and fractionation of milk fat. *European Journal of Lipid Science and Technology, 104*(11), 738-744.

Verstringe, S., Danthine, S., Blecker, C., & Dewettinck, K. (2014). Influence of a commercial monoacylglycerol on the crystallization mechanism of palm oil as compared to its pure constituents. *Food Research International, 62*, 694-700.

Verstringe, S., Dewettinck, K., Ueno, S., & Sato, K. (2014). Triacylglycerol crystal growth: templating effects of partial glycerols studied with synchrotron radiation microbeam X-ray diffraction. *Crystal Growth & Design, 14*(10), 5219-5226.

von Bonsdorff-Nikander, A., Karjalainen, M., Rantanen, J., Christiansen, L., & Yliruusi, J. (2003). Physical stability of a microcrystalline β-sitosterol suspension in oil. *European Journal of Pharmaceutical Sciences, 19*(4), 173-179.

Wright, A. J., Hartel, R. W., Narine, S. S., & Marangoni, A. G. (2000). The effect of minor components on milk fat crystallization. *Journal of the American Oil Chemists' Society, 77*(5), 463-475.

Wright, A. J., & Marangoni, A. G. (2006). Crystallization and rheological properties of milk fat. In *Advanced Dairy Chemistry Lipids*, vol. 2 (pp. 245-291). New York, NY: Springer.

Zhang, L., Hayes, D. G., Chen, G., & Zhong, Q. (2013). Transparent dispersions of milk-fat-based nanostructured lipid carriers for delivery of β-carotene. *Journal of Agricultural and Food Chemistry, 61*(39), 9435-9443.

Zychowski, L. M., Logan, A., Augustin, M. A., Kelly, A. L., Zabara, A., O'Mahony, J. A., Conn, C. E., & Auty, M. A. (2016). Effect of Phytosterols on the Crystallization Behavior of Oil-in-Water Milk Fat Emulsions. *Journal of Agricultural and Food Chemistry, 64*(34), 6546–6554.

Zychowski, L. M., Mettu, S., Dagastine, R. R., O'Mahony, J. A., & Auty, M. A. (2017). Physical and Interfacial Characterization of Phytosterols in Oil-in-Water Triacylglycerol-Based Emulsions. *Submitted to Food Structure*.

Figure Captions

Figure 1. Synchrotron (a) SAXS and (b) WAXS diffraction patterns of material references on a logarithmic scale of intensity after storage 4 °C for 24 h. Samples of (1) milk fat bulk and emulsified are included, along with crystalline and 5% (wt/wt) aqueous dispersed (2) phytosterols and (3) monoacylgylcerols (MAG). Milk fat (solid black lines), phytosterol (dashed black lines), and MAG peaks (small grey dotted lines) are distinguished by different vertical lines. The labelled peaks for phytosterols correspond to the following distances seen within formulations 1=35.6 Å; 2=17.7 Å; 3=11.7 Å; 4=9.7 Å; 5= 8.8 Å; 6=7.4 Å; 7=5.9 Å; 8=5.2 Å; 9=5.1 Å; 10=4.8 Å; 11=4.7 Å.

Figure 2. Synchrotron (a) SAXS and (b) WAXS diffraction patterns of bulk milk at 3% (wt/wt) and (c-d) 6% phytosterol (PS) enrichment with or without lecithin (LEC) or monoacylglycerols (MAG). Milk fat (solid black lines), phytosterol (dashed black lines) and MAG peaks (small grey dotted lines) are distinguished by different vertical lines. The labelled peaks for phytosterols correspond to the following distances seen within formulations: 1=35.6 Å; 2=17.7 Å; 3=11.7 Å; 4=9.7 Å; 5= 8.8 Å; 6=7.4 Å; 7=5.9 Å; 8=5.2 Å; 10=4.8 Å; 11=4.7 Å. It can be noted that no phytosterol peaks were observed in samples containing LEC or MAG in bulk samples at 3% PS enrichment.*Represents possible peak shift due to MAG crystalline peaks interference at similar Bragg distances.

Figure 3. Polarised light micrographs (partially uncrossed polarising filters) of bulk formulations with phytosterols (PS), with or without the addition of lecithin (LEC) or monoacylglycerols (MAG). The enlarged box highlights the presence of phytosterol crystals

in the 3% (wt/wt) PS sample. Scale bar = 100 µm. White Arrows highlight large milk fat spherulites.

Figure 4. Synchrotron SAXS (a) and WAXS (b) of 0.3% and (c-d) 0.6% (wt/wt) phytosterol (PS)-enriched emulsions with or without lecithin (LEC) or monoacylglycerols (MAG). The black diffraction patterns corresponds to emulsions with a $D_{(4,3)}$ of 1.0 µm with 0.2 µm shown in grey. Milk fat (solid black lines), phytosterol (dashed black lines), and MAG peaks (small grey dotted lines) are distinguished by different vertical lines. The labelled peaks for phytosterols correspond to the following distances seen within formulations 1=35.6 Å; 2=17.7 Å; 6=7.4 Å; 7=5.9 Å; 9=5.1; 10=4.8.

Tables

Table 1. Synchrotron SAXS diffraction results from bulk milk fat (MF) formulations with either added lecithin (LEC), monoacylglycerol (MAG) and/or phytosterols (PS).

Formulation	PS Conc (%)	MF Long Spacing (Å)	PS peaks	T_{onset} Final Peak (°C)	Δ H (Jg^{-1})
Bulk MF	0.0	39.4	---	23.6 ± 0.13^{ab}	-67.4 ± 0.83^{ab}
	3.0	39.5	2,4,6,7	27.3 ± 0.10^{c}	-72.0 ± 3.23^{a}
	6.0	39.5	1,2,3,4,5,6,7,8,10,11	27.2 ± 0.16^{c}	-67.8 ± 0.95^{ab}
Bulk MF + LEC	0.0	39.8	---	23.2 ± 0.08^{b}	-60.7 ± 0.56^{c}
	3.0	39.8	---	22.6 ± 0.19^{d}	-62.3 ± 0.61^{c}
	6.0	39.9	1,2,4,6,7,10,11	23.9 ± 0.16^{a}	-60.4 ± 1.76^{c}
Bulk MF + MAG	0.0	39.9	---	22.6 ± 0.06^{d}	-70.5 ± 0.42^{a}
	3.0	39.7	---	25.8 ± 0.30^{e}	-67.1 ± 1.36^{ab}
	6.0	40.1	1,2,4,6,7,10,11	26.2 ± 0.00^{e}	-68.3 ± 0.64^{ab}

PS peaks correspond as follows 1=35.6 Å; 2=17.7 Å; 3=11.7 Å; 4=9.7 Å; 5= 8.8 Å; 6=7.4 Å; 7=5.9 Å; 8=5.2 Å; 10=4.8 Å; 11=4.7 Å. Superscript letters denote significant differences in Tukey's Post Hoc Test with a $p<0.05$ and refer to data within the columns and not between different time treatments or columns.

Table 2. Changes in maximum backscattering and synchrotron diffraction results from emulsion (em) formulation (added lecithin (LEC) or monoacylglycerol (MAG) and size

Emulsion	PS Conc (%)	Droplet size ($D_{4,3}$)	Δ in BS 1-Week (%)	Δ in BS 1-Month (%)	MF Long Spacing (Å)	PS peaks
Em WPI	0.0	0.93 ± 0.06^{abc}	8.28 ± 0.85^{a}	10.4 ± 1.07^{a}	39.7	----
	0.3	0.86 ± 0.06^{bcd}	6.49 ± 1.11^{a}	9.5 ± 0.85^{ab}	39.6	6,7,9,10
	0.6	0.73 ± 0.07^{d}	6.64 ± 1.21^{a}	8.7 ± 1.07^{abc}	39.5	1,2,6,7,9,10
Em WPI + LEC	0.0	1.02 ± 0.16^{a}	2.76 ± 0.70^{bc}	10.4 ± 0.59^{a}	39.8	----
	0.3	0.99 ± 0.16^{ab}	3.76 ± 0.99^{b}	9.4 ± 1.13^{ab}	39.8	6,7,9,10
	0.6	0.95 ± 0.13^{abc}	3.69 ± 0.75^{b}	8.3 ± 0.77^{abc}	39.6	1,2,6,7,9,10
Em WPI + MAG	0.0	0.78 ± 0.06^{cd}	3.70 ± 0.97^{b}	7.4 ± 0.50^{bcd}	39.7	----
	0.3	0.79 ± 0.06^{bcd}	3.89 ± 0.47^{b}	8.7 ± 0.30^{abc}	40.0	6,7,9,10
	0.6	0.76 ± 0.05^{cd}	2.14 ± 1.00^{bc}	7.5 ± 0.65^{bcd}	40.0	1,2,6,7,9,10
Em WPI	0.0	0.21 ± 0.00^{e}	----	1.3 ± 0.32^{ef}	40.3	----
	0.3	0.20 ± 0.01^{e}	----	2.3 ± 0.33^{f}	39.9	----
	0.6	0.20 ± 0.01^{e}	----	3.5 ± 0.08^{fg}	39.7	2,6,7,9,10
Em WPI + LEC	0.0	0.18 ± 0.01^{e}	----	2.0 ± 1.19^{ef}	40.1	----
	0.3	0.19 ± 0.01^{e}	----	2.2 ± 0.58^{ef}	39.9	----
	0.6	0.17 ± 0.00^{e}	----	----	39.8	6,7,9,10
Em WPI + MAG	0.0	0.22 ± 0.00^{e}	$1.32 \pm 0.63^{cd*}$	8.8 ± 0.76^{ab}	40.3	----
	0.3	0.22 ± 0.01^{e}	----	5.7 ± 0.32^{dg}	40.2	----
	0.6	0.22 ± 0.02^{e}	----	6.5 ± 1.01^{dc}	40.2	6,7,9,10

All larger (~1.0 µm) milk fat (MF) emulsions were homogenized with 1 pass at 300 bar (top half). The smaller (~0.2 µm; bottom half) emulsion all required homogenization at 1000 bar and either 4, 3, or 5 passes for the WPI, WPI + lec, and WPI + MAG samples, respectively. The difference in backscattering data between day 0 and day 7 or 1-month is denoted as Δ in BS 1-week or Δ in BS 1-month, respectively. Phytosterol (PS) peaks within emulsions correspond as follows 1=35.6 Å; 2=17.7 Å; 3=11.7 Å; 4=9.7 Å; 5= 8.8 Å; 6=7.4 Å; 7=5.9 Å; 8=5.2 Å; 9=5.1 Å; 10=4.8 Å; 11=4.7 Å. *No statistical difference was found between this sample and samples with no change in backscattering (----); samples with no change in backscattering were recorded as 0.00 (----) and possessed the statistical label ^{d}. Superscript letters denote significant differences in Tukey's Post Hoc Test with a $p<0.05$ and refer to data within the columns and not between different time treatments or columns.

Highlights

- Phytosterol crystallisation can be minimised by lecithin and monoacylglycerols enrichment in bulk milk fat systems
- Reducing droplet size in dairy-based emulsions decreased phytosterol crystallisation
- Smaller emulsion droplets containing lecithin were the most physically stable and had minimal phytosterol crystallisation
- Results can be utilised to minimise phytosterol crystallisation in future functional food applications